Published in final edited form as:
Genesis. 2012 September ; 50(9): 711–716. doi:10.1002/dvg.22032.

Production of a Mouse Line with a Conditional *Crim1* Mutant Allele

Han Sheng Chiu[1], **J. Philippe York**[3], **Lorine Wilkinson**[2], **Pumin Zhang**[3], **Melissa H. Little**[2,§], and **David J. Pennisi**[1,§,*]

[1]School of Biomedical Sciences, The University of Queensland, Brisbane, 4072, Australia.

[2]Institute for Molecular Bioscience, The University of Queensland, Brisbane, 4072, Australia.

[3]Department of Molecular Physiology and Biophysics, Baylor College of Medicine, Houston, TX, 77030, USA.

Abstract

Crim1 is a developmentally expressed, transmembrane protein essential for normal embryonic development. We generated mice engineered to contain a *Crim1* conditional null allele by flanking exons three and four of *Crim1* with unidirectional LoxP sites. After crossing $Crim1^{+/FLOX}$ mice with a CMV-Cre line, a $Crim1^{+/\Delta flox}$ colony was established after germline transmission of the deleted allele. We then analyzed genomic DNA, mRNA transcripts, and protein expression from $Crim1^{\Delta flox/\Delta flox}$ null mice to confirm the nature of the genomic lesion. $Crim1^{\Delta flox/\Delta flox}$ mice displayed phenotypes similar to those previously described for a *Crim1* gene-trap mutant, $Crim1^{KST264/KST264}$, including perinatal lethality, digit syndactyly, eye, and kidney abnormalities, with varying penetrance and severity. The production of a conditional mutant allele represents a valuable resource for the study of the tissue-specific roles for *Crim1*, and for understanding the pleimorphic phenotypes associated with *Crim1* mutation.

Keywords

cysteine rich transmembrane BMP regulator 1 (chordin-like); FLOXed allele; mouse mutant; renal development; organogenesis

---

Crim1 encodes a developmentally expressed transmembrane protein that contains six von Willebrand Factor-C (vWFC)-like cysteine-rich repeats (CRRs) similar to the BMP-regulating protein, Chordin (Georgas *et al.*, 2000; Kolle *et al.*, 2000; Pennisi *et al.*, 2007). Crim1 can bind a broad range of cystine-knot growth factors, including TGFβ, BMP, VEGF, and PDGF family members, and such binding occurs only when Crim1 is co-expressed in the same cell as the growth factor (Wilkinson *et al.*, 2003). Recent studies have further supported the idea that Crim1 has a role in antagonizing BMP function, including the *Drosophila* homolog of Crim1, Crimpy (James and Broihier, 2011; Zhang *et al.*, 2011). Our analysis of a *Crim1* gene-trap line mutant, $Crim1^{KST264}$, found that homozygous $Crim1^{KST264/KST264}$ mice died perinatally on a C57Bl6 genetic background and displayed abnormal kidney, eye, limb and placental development (Pennisi *et al.*, 2012; Pennisi *et al.*, 2007). When bred onto a mixed C57Bl6/CD1 background, $Crim1^{KST264/KST264}$ mice display a similar array of phenotypes, but can survive to adulthood (with reduced viability;

*Correspondence to: David Pennisi, School of Biomedical Sciences, The University of Queensland, Brisbane, 4072, Australia. d.pennisi@uq.edu.au.
§DJP and MHL are senior co-authors on this work.

(Wilkinson *et al.*, 2007)). Exon 2-minus transcripts are produced at low levels from the *Crim1*^{KST264} locus and are predicted to produce in-frame transcripts, suggesting the *Crim1*^{KST264} may be a hypomorphic or gain-of-function mutation (Pennisi *et al.*, 2007).

Our previous work showed that Crim1 binds and regulates VEGF-A activity *in vivo*, with *Crim1*$^{KST264/KST264}$ displaying excessive VEGF-A diffusion away from the podocytes of the renal glomerulus (where Crim1 and VEGF-A are co-expressed), resulting in increased activation of VEGFR-2 in adjacent vascular endothelial cells (Wilkinson *et al.*, 2007). Crim1 is expressed in numerous cell types during development and homeostasis, and the activity of numerous growth factors derived from multiple cell types is likely to be perturbed upon mutation of Crim1 (Georgas *et al.*, 2000; Kolle *et al.*, 2000; Pennisi *et al.*, 2007; Wilkinson *et al.*, 2007; Wilkinson *et al.*, 2003). Thus, analysis of the pleiomorphic phenotypes observed in *Crim1*$^{KST264/KST264}$ mice is problematic. To overcome some of these difficulties, and to facilitate investigations on tissue-specific and postnatal roles for *Crim1* in embryonic development and disease, we generated a *Crim1* conditional knock-out mouse line by flanking exons 3 and 4 with unidirectional LoxP sites (*Crim1*^{FLOX} allele, Figure 1).

PCR analysis of genomic DNA was used to confirm the production of the mutant *Crim1* alleles and to establish a convenient method for genotyping (Figure 2 a–c). *Crim1*$^{FLOX/FLOX}$ mice on C57Bl6 and CD1 genetic backgrounds were viable, fertile, and displayed no anomalous phenotypes relative to *Crim1*$^{+/FLOX}$ or *Crim1*$^{+/+}$ littermates (not shown). Colonies of *Crim1*$^{\Delta flox}$ mice were established after breeding *Crim1*^{FLOX} mice with a CMV-Cre line. We then confirmed that exons 3 and 4 were deleted in *Crim1*$^{\Delta flox}$ allele. PCR was performed on the genomic DNA (gDNA) of embryonic samples of various genotypes using primer pairs specific for *Crim1* exons 1 and 2 (5′ to the FLOXed region), exon 3 (within the FLOXed region), and exon 11 (3′ to the FLOXed region). Amplicons for all exons tested were observed for *Crim1*$^{+/+}$ and *Crim1*$^{+/\Delta flox}$ samples. However, only exons 1, 2 and 11 were observed in *Crim1*$^{\Delta flox/\Delta flox}$ samples (Figure 2 d).

Characterization of the transcripts from the *Crim1*$^{\Delta flox}$ locus was performed using RT-PCR on mRNA from embryonic kidney samples. Full-length transcripts were observed in *Crim1*$^{+/+}$ samples, however we only found a shorter transcript lacking the regions encoded by exons 3 and 4 in *Crim1*$^{\Delta flox/\Delta flox}$ samples (Figure 3 a). In addition, no transcripts from exon 3 could be detected by real-time PCR with exon-specific primer pairs on whole kidney cDNA (qRT-PCR), further confirming the Cre-mediated deletion of the genomic region in *Crim1*$^{\Delta flox/\Delta flox}$ mice (Figure 3 b). The *Crim1*$^{\Delta flox}$ transcript lacks the region encoded by exons 3 and 4, that produces an out-of-frame transcript resulting in a premature stop codon, and is predicted to be non-functional. Section immunohistochemistry was then performed with an anti-Crim1 antibody on kidneys from *Crim1*$^{+/\Delta flox}$ and *Crim1*$^{\Delta flox/\Delta flox}$ 16dpc embryos. As expected, we observed immunostaining signal in *Crim1*$^{+/\Delta flox}$ samples. However, no signal was observed in *Crim1*$^{\Delta flox/\Delta flox}$ samples, consistent with the lack of a functional protein translated from *Crim1*$^{\Delta flox}$ transcripts (Figure 3 c–e).

We intercrossed *Crim1*$^{+/\Delta flox}$ mice to examine the nature of the conditional *Crim1* mutation. From matings with C57Bl6 background, we did not observe *Crim1*$^{\Delta flox/\Delta flox}$ pups (Table 1). By contrast, from matings of *Crim1*$^{+/\Delta flox}$ mice with a CD1 background, *Crim1*$^{\Delta flox/\Delta flox}$ pups were observed at a frequency less than would be expected based on Mendelian ratios (approximately 62.5% of expected values; Table 1). The frequency of the genotypes of embryos at different stages was then analyzed after intercrosses of *Crim1*$^{+/\Delta flox}$ mice with a C57Bl6 background (Table 2). Although there may be a trend of reduced viability of *Crim1*$^{\Delta flox/\Delta flox}$ embryos, a statistically significant difference in the numbers of *Crim1*$^{\Delta flox/\Delta flox}$ mice was not observed until the postnatal period. *Crim1*$^{\Delta flox/\Delta flox}$ embryos displayed a range of phenotypes, including peridermal blebbing evident at 12.5dpc and

13.5dpc (Figure 4 a, b); mild digit syndactyly from 13.5dpc (Figure 4 c–f); eye hypoplasia from 13.5dpc (Figure 4 g, h); renal hypoplasia (Figure i, j) and glomerular dysgenesis (Figure 4 k–n); and a proportion displayed widespread edema (Figure 4 o, p). *Crim1*$^{\Delta flox/\Delta flox}$ mice, like the previously described *Crim1*$^{KST264/KST264}$ mice, are characterized by a pleiomorphic phenotype affecting numerous organ systems in development. These include the perinatal lethality on a C57Bl6 background, renal, eye, and digit dysgenesis, and peridermal blebbing, are consistent with those described in *Crim1*$^{KST264/KST264}$ embryos (Pennisi *et al.*, 2007). However, a widespread edema was not observed in *Crim1*$^{KST264/KST264}$ embryos. Like *Crim1*$^{KST264/KST264}$ mice, *Crim1*$^{\Delta flox/\Delta flox}$ mice on a predominantly CD1 genetic background can survive postnatally, albeit at reduced viability (Wilkinson *et al.*, 2007).

It is noteworthy that, although similar phenotypes were observed among *Crim1*$^{\Delta flox/\Delta flox}$ embryos and mice, relative to that described for the *Crim1*$^{KST264/KST264}$ mutation, there appeared to be some difference in the severity and/or the penetrance of phenotypes. This likely reflects the differences in the *Crim1*$^{\Delta flox}$ and *Crim1*^{KST264} mutations. Transcripts from the *Crim1*^{KST264} allele include a fusion of the coding region of Crim1 exon 1 and the β-Geo from the gene-trap and an in-frame exon 2-minus splice variant (Pennisi *et al.*, 2007). This latter transcript is also detected in wild-type embryos as a minor splice variant in numerous developing organs (Pennisi *et al.*, 2007). Importantly, RT-PCR analyses on transcription from the *Crim1*$^{\Delta flox}$ allele confirm an out-of-frame transcript lacking exon 3 and exon 4. Although unlikely, an alternative explanation remains a formal possibility; as there have been less than ten generations of backcrossing, it is possible that some residual genetic material from the chimeric founders may contribute sufficient genetic variability. The production of a mouse line with a conditional *Crim1*^{FLOX} allele will be an invaluable tool in dissecting the tissue-specific contribution of Crim1 to the development of different organ systems. Furthermore, by the use of inducible Cre-expressing lines, a conditional null *Crim1* allele will allow the examination of the role of *Crim1* in postnatal development or disease by circumventing confounding embryonic defects.

Materials and Methods

Generation of a FLOXed *Crim1* allele *Crim1*$^{+/FLOX}$

A targeting vector was produced by recombinant engineering methods (Zhang *et al.*, 2002) to flank exons 3 and 4 of the mouse Crim1 gene with unidirectional LoxP sites (Figure 1), and was then introduced into E14 embryonic stem (ES) cells (Wakayama *et al.*, 1999). Drug-resistant ES cell clones were screened for homologous recombinants by Southern blotting of genomic DNA after digestion with *Bam*H1. After transfer to membranes, blots were probed with pooled 5′ and 3′ flanking probes (Figure 1). The probes were generated by PCR with the following primer pairs: 5′ Probe-For, 5′-GTCTTACGCAGCAGCCGAAG-3′ and 5′ Probe-Rev, 5′-GAACACAAGTGGATCAGG-3′; 3′ Probe-For, 5′-CCAAGTTTGTGGCACAGTG-3′ and 3′ Probe-Rev, 5′-CCCACATTTACAGAGGCCG-3′. Successful homologous recombinants ES cells were injected into C57BL6 blastocysts and transferred to pseudopregnant mothers, and chimeric offspring were bred for germline transmission of the *Crim1*^{FLOX} allele. The *Crim1*^{FLOX} mouse line will be made available through the Australian Phenomics Network (www.australianphenomics.org.au).

Crim1$^{\Delta flox}$ mice were established after mating *Crim1*$^{+/FLOX}$ and CMV-Cre mice to produce germline deletion of exons 3 and 4 of the *Crim1* gene. The CMV-Cre mouse line has been described (Su *et al.*, 2002) and was genotyped by PCR on genomic DNA to detect the Cre transgene with the following primers: CRE-For, 5′-CCTGGAAAATGCTTCTGTCCG-3′ and CRE-Rev, 5′-CAGGGTGTTATAAGCAATCCC-3′. *Crim1*^{FLOX} and *Crim1*$^{\Delta flox}$ mice were backcrossed onto the inbred C57Bl6 genetic background for more than five

generations. *Crim1*$^{\Delta flox}$ mice were also backcrossed onto the outbred CD1 genetic background for more than five generations.

Genotyping

Genotyping of *Crim1*^{FLOX} and *Crim1*$^{\Delta flox}$ mice was performed by PCR on genomic DNA with the following primers: F2, 5′-TTCTTGGGTTCACAGTTAGTCC-3′; B3, 5′-AATGGAATCTTCAGGGCAAC-3′; PGK-Rev, 5′-GAGACGTGCTACTTCCATTTGTC-3′. Primer pair F2 and B3 will yield an amplicon of 389bp (wild-type allele) or 471bp (*Crim1*^{FLOX} allele). Primer pair F2 and PGK-Rev will yield an amplicon of ~500bp only from a *Crim1*$^{\Delta flox}$ allele.

Reverse Transcription-Polymerase Chain Reaction (RT-PCR) and Transcript Analyses

Reverse Transcriptase-Polymerase Chain Reaction (RT-PCR) was performed as previously described (Pennisi *et al.*, 2007) using the following primers; Exon1 Forward, 5′-ACGAGTCCAAGTGCGAGGAG-3′; Exon5 Reverse, 5′-AAAACCACATAAGCCAGAGAGAC-3′. Real-time PCR was performed as previously described (Pennisi *et al.*, 2007) on three samples of each genotype, using the mouse *Crim1* exon-specific and mouse TFIID primer pairs detailed therein. Expression levels were expressed as a ratio of TFIID values. The qRT-PCR data presented are representative of at least three independent experiments.

Embryo Sample Preparation

Skeletal preparations were performed as previously described (Pennisi *et al.*, 2007). Hematoxylin and eosin staining was performed using standard procedures on 7μm sections of paraformaldehyed-fixed, paraffin-embedded samples. Section immunohistochemistry was performed on paraformaldehyde-fixed, paraffin-embedded samples as described (Pennisi and Mikawa, 2009) with an anti-CRIM1 antibody (HPA000556, Sigma) and counterstained with hematoxylin. This antibody has been used to detect CRIM1 in formalin-fixed, paraffin-embedded renal tissue (Nyström *et al.*, 2009). The immunogen sequence provided for the anti-CRIM1 antibody incorporates amino acids coded by *Crim1* exon 1 (10 amino acids), exon 2 (58 amino acids), and exon 3 (39 amino acids).

Data Documentation

Digital whole-mount images were captured using an Olympus SZX-12 stereo-microscope and section images were captured using an Olympus BX-51 BF/DF slide microscope with DP Controller software (Olympus, Japan). Images were adjusted for colour levels, brightness and contrast, and figures compiled, using Adobe Photoshop software.

Statistical Analyses

The statistical significance of deviation from expected Mendelian ratios (1:2:1) of offspring or embryos from *Crim1*$^{+/\Delta flox}$ intercrosses was determined using Chi-square tests. For determining the statistical significance in the change of mRNA expression levels to *Crim1*$^{+/+}$ samples, an unpaired, two-tailed Student's t-test.

Acknowledgments

We thank the staff of The University of Queensland Biological Resources animal facilities for support. This study conformed to the Institute's Animal Ethics Committee guidelines for animal use in research. This work was funded by Project Grants from the National Health and Medical Research Council of Australia to DJP (grant number 631658) and MHL (grant number 455972), and NIH funding to PZ (U01 DK070214).

References

Georgas K, Bowles J, Yamada T, Koopman P, Little MH. Characterisation of Crim1 expression in the developing mouse urogenital tract reveals a sexually dimorphic gonadal expression pattern. Developmental Dynamics. 2000; 219:582–587. [PubMed: 11084657]

James RE, Broihier HT. Crimpy inhibits the BMP homolog Gbb in motoneurons to enable proper growth control at the Drosophila neuromuscular junction. Development. 2011; 138:3273–3286. [PubMed: 21750037]

Kolle G, Georgas K, Holmes GP, Little MH, Yamada T. CRIM1, a novel gene encoding a cysteine-rich repeat protein, is developmentally regulated and implicated in vertebrate CNS development and organogenesis. Mechanisms of Development. 2000; 90:181–193. [PubMed: 10642437]

Nyström J, Hultenby K, Ek S, Sjölund J, Axelson H, Jirström K, Saleem MA, Nilsson K, Johansson ME. CRIM1 is localized to the podocyte filtration slit diaphragm of the adult human kidney. Nephrology Dialysis Transplantation. 2009; 24:2038–2044.

Pennisi DJ, Kinna G, Chiu HS, Simmons DG, Wilkinson L, Little MH. Crim1 has an essential role in glycogen trophoblast cell and sinusoidal-trophoblast giant cell development in the placenta. Placenta. 2012; 33:175–182. [PubMed: 22225908]

Pennisi DJ, Mikawa T. FGFR-1 is required by epicardium-derived cells for myocardial invasion and correct coronary vascular lineage differentiation. Developmental Biology. 2009; 328:148–159. [PubMed: 19389363]

Pennisi DJ, Wilkinson L, Kolle G, Sohaskey ML, Gillinder K, Piper MJ, McAvoy JW, Lovicu FJ, Little MH. Crim1KST264/KST264 mice display a disruption of the Crim1 gene resulting in perinatal lethality with defects in multiple organ systems. Developmental Dynamics. 2007; 236:502–511. [PubMed: 17106887]

Su H, Mills AA, Wang X, Bradley A. A targeted X-linked CMV-Cre line. Genesis. 2002; 32:187–188. [PubMed: 11857817]

Wakayama T, Rodriguez I, Perry AC, Yanagimachi R, Mombaerts P. Mice cloned from embryonic stem cells. Proceedings of the National Academy of Sciences USA. 1999; 96:14984–14989.

Wilkinson L, Gilbert T, Kinna G, Ruta LA, Pennisi D, Kett M, Little MH. Crim1KST264/KST264 mice implicate Crim1 in the regulation of vascular endothelial growth factor-A activity during glomerular vascular development. Journal of the American Society of Nephrology. 2007; 18:1697–1708. [PubMed: 17460146]

Wilkinson L, Kolle G, Wen D, Piper M, Scott J, Little M. CRIM1 regulates the rate of processing and delivery of bone morphogenetic proteins to the cell surface. Journal of Biological Chemistry. 2003; 278:34181–34188. [PubMed: 12805376]

Zhang JF, Fu WM, He ML, Xie WD, Lv Q, Wan G, Li G, Wang H, Lu G, Hu X, Jiang S, Li JN, Lin MC, Zhang YO, Kung H. MiRNA-20a promotes osteogenic differentiation of human mesenchymal stem cells by co-regulating BMP signaling. RNA Biology. 2011; 8:829–838. [PubMed: 21743293]

Zhang P, Li MZ, Elledge SJ. Towards genetic genome projects: genomic library screening and gene-targeting vector construction in a single step. Nature Genetics. 2002; 30:31–39. [PubMed: 11753384]

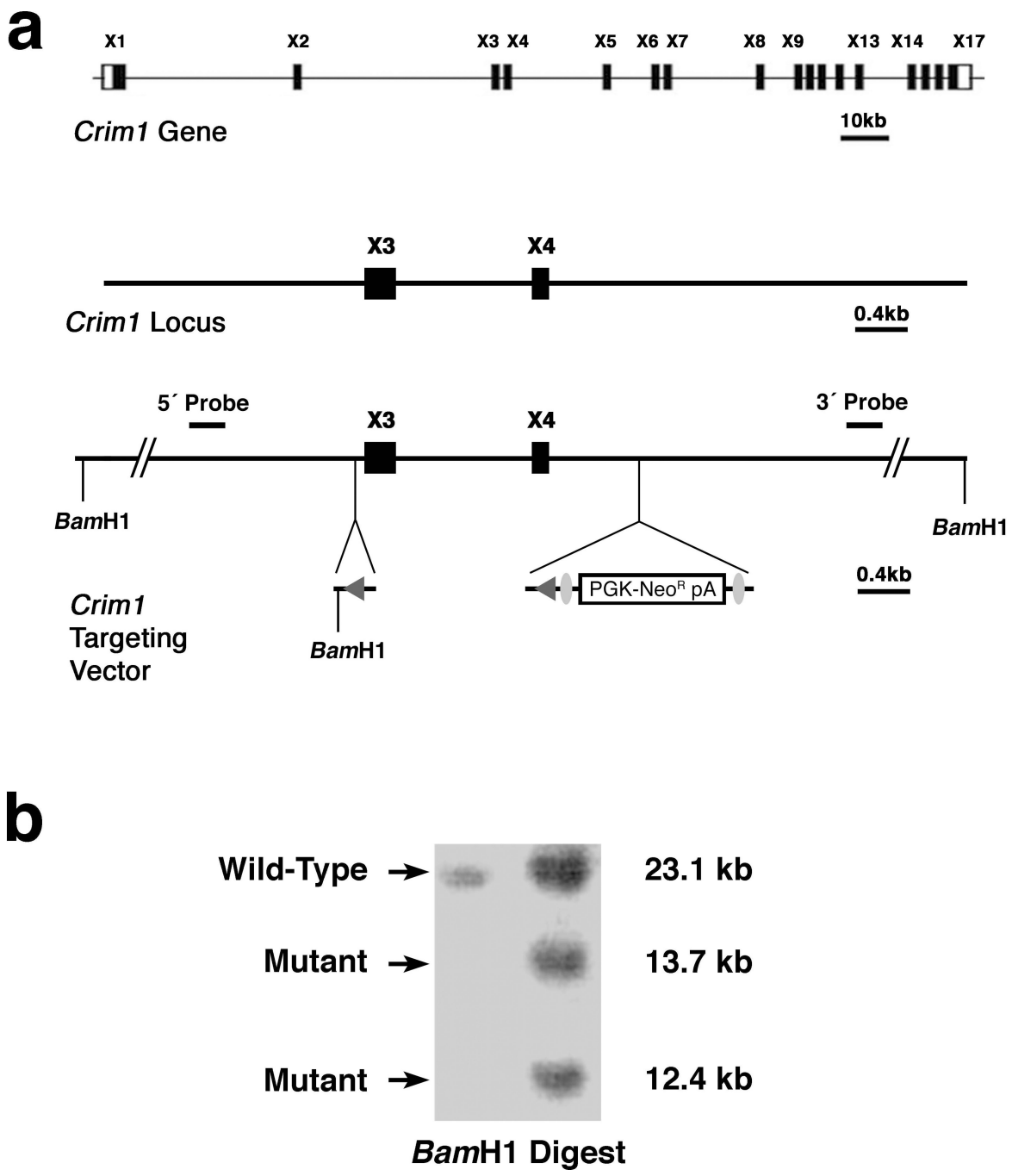

Figure 1.

Generation of a conditional mutant *Crim1* allele. **(a)** Ideogram of the targeting strategy to produce the *Crim1*^{FLOX} conditional allele. Shown are the *Crim1* gene (exons not to scale), the region including exon 3 and exon 4 of the wild-type *Crim1* locus to be targeted, and the targeting vector showing the introduced *Bam*H1 restriction site and the approximate sites of the 5´ and 3´ flanking probes used for screening ES cell clones. The unidirectional LoxP sites are denoted by triangles. **(b)** Southern blotting was performed on resistant ES cell clone genomic DNA after *Bam*H1 digestion to screen for homologous recombinants. 5´ and 3´ flanking probes were pooled for hybridization of membranes. Shown is an autoradiograph

with a successful homologous recombinant (right lane). The size of the wild-type and mutant bands are indicated.

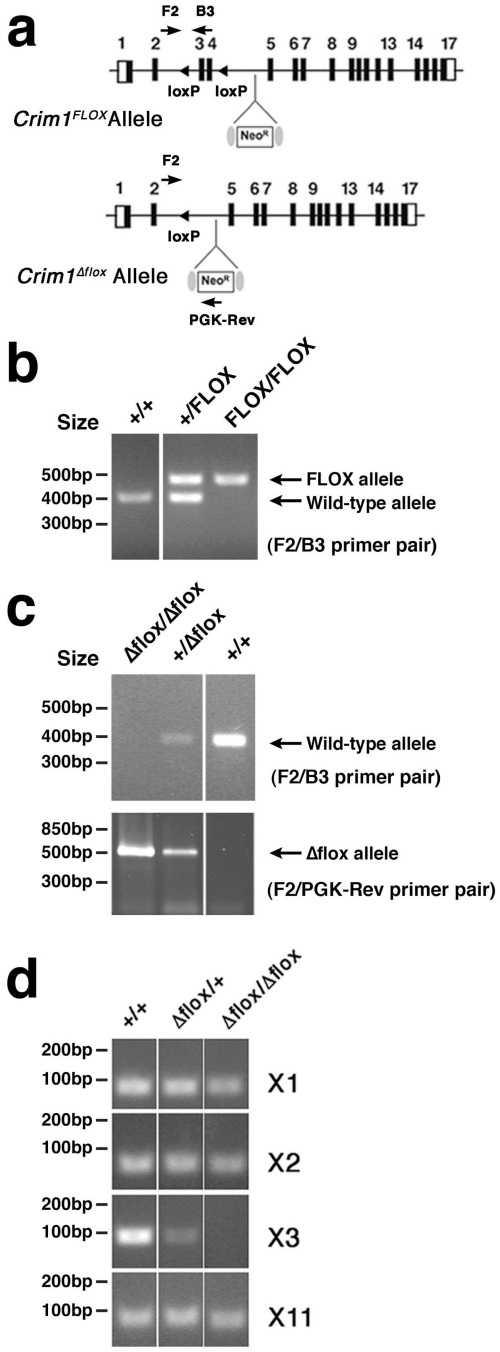

Figure 2.

Genotyping and genomic DNA analysis of mutant *Crim1* alleles. **(a)** Ideogram of $Crim1^{FLOX}$ conditional and $Crim1^{\Delta flox}$ mutant alleles showing the primers used for genotyping (arrows) and LoxP sites (triangles). **(b)** PCR genotyping for the $Crim1^{FLOX}$ conditional allele was performed with the primers F2 and B3. Note the larger amplicon from the $Crim1^{FLOX}$ allele relative to wild-type allele due to the presence of the upstream LoxP site (and targeting vector sequence). **(c)** Genotyping to discriminate between $Crim1^{+/+}$, $Crim1^{+/\Delta flox}$, and $Crim1^{\Delta flox/\Delta flox}$ samples after intercrossing $Crim1^{+/\Delta flox}$ mice was performed with two PCR reactions; F2 and B3 to detect the wild-type allele, and F2 and

PGK-Rev to detect the *Crim1*$^{\Delta flox}$ allele. **(d)** PCR on genomic DNA of *Crim1*$^{+/+}$, *Crim1*$^{+/\Delta flox}$, and *Crim1*$^{\Delta flox/\Delta flox}$ samples with primer pairs to amplify exons 1, 2, 3, and 11 of *Crim1* confirms the desired genomic lesion after Cre-mediated deletion. Note the absence of an exon 3-specific amplicon in *Crim1*$^{\Delta flox/\Delta flox}$ samples and the presence of amplicons from flanking genomic regions.

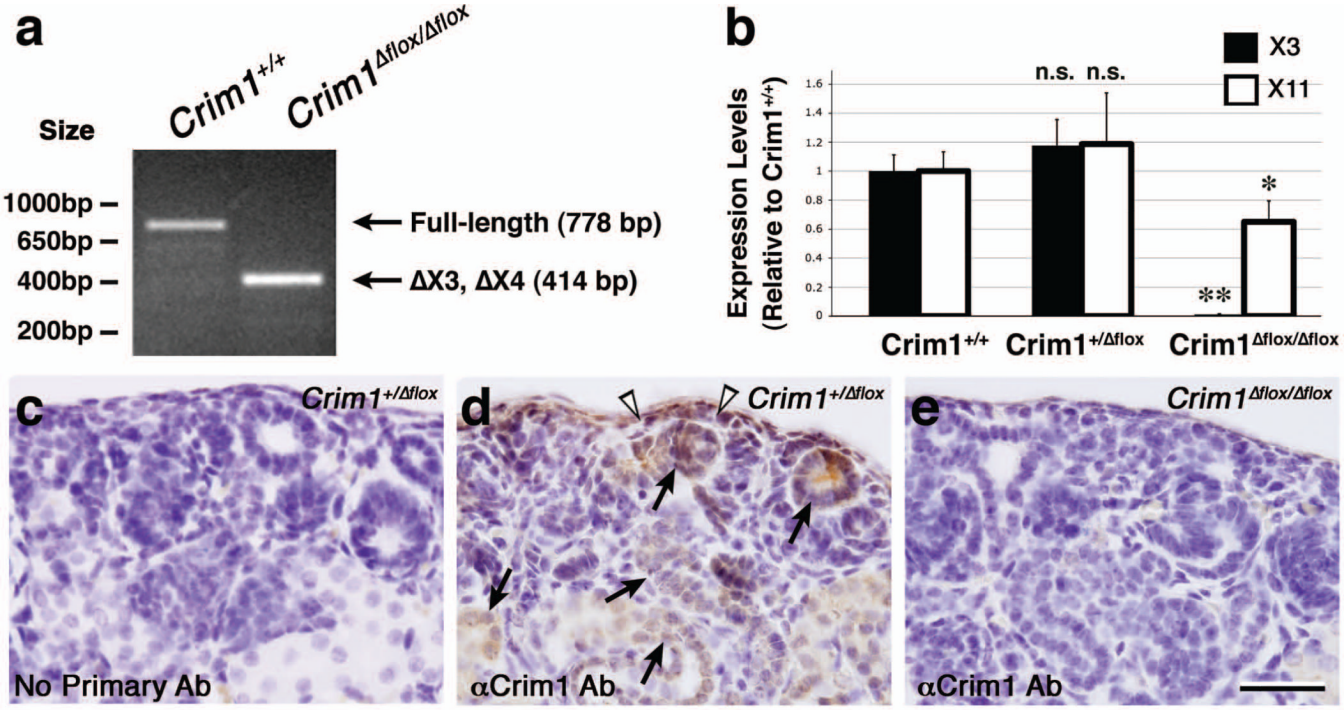

Figure 3.

Confirmation of the mutant nature of the *Crim1*$^{\Delta flox}$ allele. **(a)** Qualitative RT-PCR analysis of *Crim1* transcripts from total 15.5dpc kidney mRNA from *Crim1*$^{+/+}$ and *Crim1*$^{\Delta flox/\Delta flox}$ embryos. Primers were designed to amplify transcripts encoded from exon 1 to exon 5. Note the full-length transcript encoded by exons 1 to 5 in the *Crim1*$^{+/+}$ sample. In the *Crim1*$^{\Delta flox/\Delta flox}$ sample, however, a shorter transcript is evident lacking the regions encoded by exon 3 and exon 4, consistent with the Cre-mediated deletion of the conditional allele. Importantly, these transcripts are predicted to be out-of-frame and non-functional. **(b)** Real-time PCR (qRT-PCR) analysis of *Crim1* transcripts from *Crim1*$^{+/+}$, *Crim1*$^{+/\Delta flox}$, and *Crim1*$^{\Delta flox/\Delta flox}$ total 15.5dpc kidney mRNA. Expression levels were normalized with that of TFIID and expressed as a fraction of *Crim1*$^{+/+}$ values. Note the absence of exon 3-encoded transcripts (closed boxes) in *Crim1*$^{\Delta flox/\Delta flox}$ samples, further confirming the nature of the transcript from the mutant allele. Error bars represent standard deviation of the mean. n.s., not significant; *, $P < 0.05$; **, $P < 0.01$. **(c–e)** Micrographs after anti-Crim1 section immunohistochemistry of 16dpc kidney from *Crim1*$^{+/\Delta flox}$ (d) and *Crim1*$^{\Delta flox/\Delta flox}$ (e) embryos. Note the positive immunostaining (brown signal) in the nephrogenic mesenchyme (arrowheads) and tubular structures (arrows) of the *Crim1*$^{+/\Delta flox}$ kidney (d). There was a lack of immunostaining in the *Crim1*$^{+/\Delta flox}$ control in the absence of a primary antibody (c) and the *Crim1*$^{\Delta flox/\Delta flox}$ sample with the anti-Crim1 antibody (e). Scale bar, 100μm.

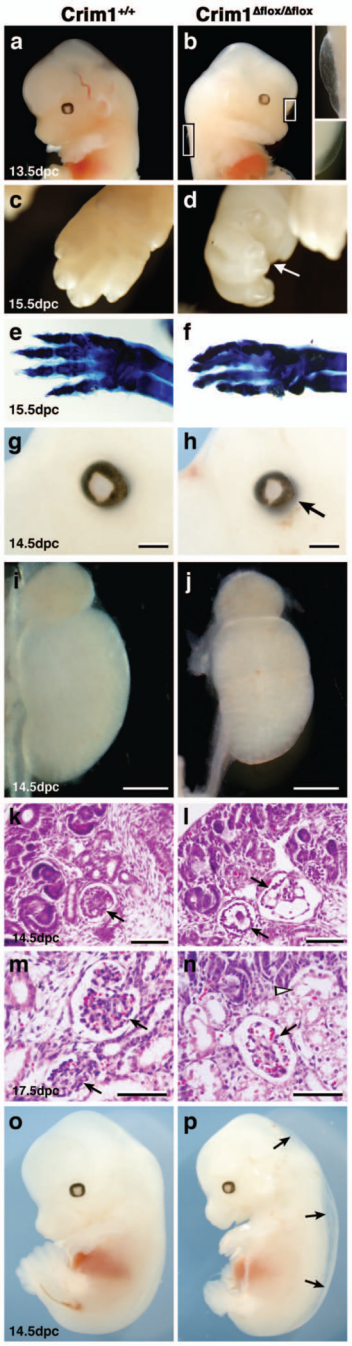

Figure 4.

The phenotype of *Crim1*$^{\Delta flox/\Delta flox}$ embryos resembles that of *Crim1*$^{KST264/KST264}$ embryos. **(a, b)** Micrographs of *Crim1*$^{+/+}$ (a) and *Crim1*$^{\Delta flox/\Delta flox}$ (b) 13.5dpc embryos viewed in whole-mount. Note the peridermal blebbing in the *Crim1*$^{\Delta flox/\Delta flox}$ embryo (insets, enlarged views of the boxed areas in b). **(c, d)** Micrographs of *Crim1*$^{+/+}$ (c) and *Crim1*$^{\Delta flox/\Delta flox}$ (d) 15.5dpc embryo forelimbs viewed in whole-mount. Note the mild digit syndactyly in the forelimb of the *Crim1*$^{\Delta flox/\Delta flox}$ 15.5dpc embryo (arrow, d). **(e, f)** Micrographs of skeletal preparations of the *Crim1*$^{+/+}$ (e) and *Crim1*$^{\Delta flox/\Delta flox}$ (f) 15.5dpc embryonic forelimbs shown in c and d, respectively. **(g, h)** Micrographs of *Crim1*$^{+/+}$ (g) and *Crim1*$^{\Delta flox/\Delta flox}$ (h)

14.5dpc embryonic heads viewed in whole-mount. Note the eye dysgenesis in the *Crim1*$^{\Delta flox/\Delta flox}$ 14.5dpc embryo (arrow, h) relative to the *Crim1*$^{+/+}$ control. **(i, j)** Micrographs of *Crim1*$^{+/+}$ (i) and *Crim1*$^{\Delta flox/\Delta flox}$ (j) 14.5dpc embryonic kidneys viewed in whole-mount. Note the reduced size of the kidney from the *Crim1*$^{\Delta flox/\Delta flox}$ embryo. **(k, l)** Micrographs of hematoxylin and eosin-stained sections of 14.5dpc kidneys. Note the poorly formed glomeruli with distended capillaries in *Crim1*$^{\Delta flox/\Delta flox}$ kidneys (arrows, l) compared with that of a well-developed glomerulus in a *Crim1*$^{+/+}$ kidney (arrow, k). **(m, n)** Micrographs of hematoxylin and eosin-stained sections of 17.5dpc kidneys. An example of a malformed glomerulus in a *Crim1*$^{\Delta flox/\Delta flox}$ kidney (arrow, n) compared with *Crim1*$^{+/+}$ kidney (arrows, m). In the 17.5dpc *Crim1*$^{\Delta flox/\Delta flox}$ kidneys, there is also evidence of a malformed tubule or a severely affected glomerulus (arrowhead, n). **(o, p)** Micrographs of *Crim1*$^{+/+}$ (o) and *Crim1*$^{\Delta flox/\Delta flox}$ (p) 14.5dpc embryos viewed in whole-mount. Note the edema in the *Crim1*$^{\Delta flox/\Delta flox}$ embryo (arrows, n). Scale bars; g–j, 500μm; k–n, 100μm.

Table 1

The frequency of the genotypes of pups from intercrosses of *Crim1*$^{+/\Delta flox}$ mice with a C57Bl6 or CD1 genetic background.

		Number of Pups				
Genetic back-ground	**# Pups (# Litters)**	***Crim1*$^{+/+}$**	***Crim1*$^{+/\Delta flox}$**	***Crim1*$^{\Delta flox/\Delta flox}$**	**Chi-squared**	**P value**
C57Bl6	29 (6)	11	18	0	10.0344	0.0066
CD1	319 (26)	83	181	55	10.7115	0.0047

Table 2

The frequency of the genotypes of embryos at different stages from intercrosses of *Crim1*$^{+/\Delta flox}$ mice with a C57Bl6 background.

			Number of Embryos (%)					
Stage	**# Embryos (# Litters)**	**# *Crim1* $^{\Delta flox/\Delta flox}$ with phenotype**	***Crim1*** $^{+/+}$	***Crim1*** $^{+/\Delta flox}$	***Crim1*** $^{\Delta flox/\Delta flox}$	**Resorbed Embryos (not genotped)**	**Chi-squared**	**P value**
9.5dpc	121 (19)	0	31	64	26	2	0.8181	0.6643
10.5dpc	40 (5)	0	11	24	5	0	3.3999	0.1827
12.5dpc	58 (7)	5	22	23	13	6	5.2758	0.0715
13.5dpc	137 (16)	31	34	62	41	11	1.9489	0.3774
14.5dpc	27 (4)	5	8	11	8	1	0.9259	0.6294
15.5dpc	34 (6)	4	9	15	10	4	0.5294	0.7674
16.5dpc	27 (4)	3	8	14	5	2	0.7037	0.7034
17.5dpc	14 (2)	0	4	9	1	0	2.4285	0.297